

Article

An Optimization Design of Hybrid Parking Lots in an Automated Environment

Taolüe Chen  and Chao Sun *

School of Automotive and Traffic Engineering, Jiangsu University, Zhenjiang 212013, China; 3210402022@stmail.ujs.edu.cn

* Correspondence: chaosun@ujs.edu.cn; Tel.: +86-13276613357

Abstract: This paper explores the minimum lateral parking distance and parking acceleration/deceleration distance of vehicles to improve the efficiency of automated valet parking (AVP) lots and save urban land. Specifically, the paper focuses on designing parking lots for automated guided vehicles (AGVs) and their parking attributes. To ensure AGV accessibility and maximize AVP capacity, graph theories and unique path-driving methods are used in designing mobile priority parking lots and decision spaces. Additionally, the paper proposes an optimization design for parking lots with obstacles, considering the layout of load-bearing columns and charging resources for electric vehicles in underground parking lots. The article further proposes an optimization design for hybrid parking lots based on spatio-temporal resource conversion in traffic design and the principle of traffic separation in traffic control since hybrid parking lots that accommodate both conventional vehicles and AGVs are crucial to the future development of urban parking lots. The experimental results show that the proposed optimization design for urban parking lots in automated environments is superior to the traditional parking lots design in terms of capacity and density. This paper provides an optimal layout scheme of urban parking lots in multiple scenarios, which can improve the service level of urban static traffic systems.

Keywords: hybrid parking; automated valet parking (AVP); high-density parking; automated guided vehicle (AGV)



Citation: Chen, T.; Sun, C. An Optimization Design of Hybrid Parking Lots in an Automated Environment. *Sustainability* **2023**, *15*, 15475. <https://doi.org/10.3390/su152115475>

Academic Editors: Jie Ma, Jingxu Chen and Xinlian Yu

Received: 16 October 2023
Revised: 23 October 2023
Accepted: 30 October 2023
Published: 31 October 2023



Copyright: © 2023 by the authors. Licensee MDPI, Basel, Switzerland. This article is an open access article distributed under the terms and conditions of the Creative Commons Attribution (CC BY) license (<https://creativecommons.org/licenses/by/4.0/>).

1. Introduction

Automated vehicles are a popular research topic in intelligent transportation systems, and their widespread adoption will bring new opportunities for urban transportation development. Xie et al. (2022) consider automated valet parking (AVP) to be one of the most advanced technologies for improving parking efficiency and safety [1]. The number of cars in urban areas has increased significantly in recent years. As a result, a constant rise in demand for parking has led to traffic congestion in traditional parking lots. However, with the advent of innovative technologies and the growing popularity of automated vehicles, there is potential for a significant change in the demand for parking. Many scholars believe that high-density automated valet parking could provide new ideas and solutions for urban parking, making it more efficient and less congested.

The benefits of self-driving cars include reducing the personnel burden, optimizing the parking lot location, improving parking efficiency, and increasing land utilization. For example, Zhang et al. (2021) believe that automated valet parking (AVP) systems based on automated guided vehicles (AGVs) can reduce the workload and improve the efficiency to a certain extent due to their fully automatic control and operation [2]. With the advancement of urbanization, the problem of insufficient parking space in cities has become increasingly prominent. Chen et al. (2021) adopt high-density parking lots equipped with parking robots, which can significantly improve the land utilization rate of parking lots [3]. Bahrami et al. (2020) argue that automated vehicles can park themselves and be stacked on each

other, like valet parking, thereby improving land utilization [4]. Experimental results designed by Kang et al. (2022) show that 14.60% to 32.27% (scenario-based) of the area currently used as parking space for automated vehicles can be reused [5].

Another significant advantage of automated vehicles is the reduced cost. For example, Zakharenko et al. (2016) suggest that automated vehicles reduce the cost of commuting per kilometer [6]. In Millard-Ball's study, automated vehicles could more than double the number of vehicles entering and leaving dense urban cores, reducing effective parking costs by 90% [7]. In addition, the implementation of automated vehicles (AVs) can provide many advantages, such as increased network capacity and fewer accidents.

Previous studies by some authors have envisioned parking schemes to increase the density of parked vehicles or the equivalent of increasing parking capacity. Ferreira et al. (2014) first proposed high-density parking for automated vehicles [8]. Zaerpour et al. (2017) investigated living cube compact storage systems that do not require moving channels to solve this space shortage [9]. Nourinejad et al. (2018) designed an optimal parking lot layout, treating each island in the parking lot as a queuing system. They found that self-driving car parking could reduce parking demand by an average of 62% and by as much as 87% [10]. The parking lot designed by Azevedo et al. (2020) utilizes electrification and low levels of driving automation to more than double the density of cars parked in a given area compared to traditional parking lots [11]. Naji et al. (2022) used a developed real-time VHDL (VHSIC Hardware Description Language) algorithm to generate various candidate patterns, providing the best solution with performance metrics. Based on simulation and experimental results, the AVPS system can detect and recognize parking patterns in advance. This combination describes a complete implementation based on a specific FPGA (Field-programmable Gate Array) card on a mobile robot such as a car [12].

Yalcin et al. (2018) proposed the grid-based modeling of parking lots through a puzzle-based storage system consisting of dense cell loads on a square grid [13]. In the same research on parking grid modeling, Kim et al. (2022) proposed an intelligent parking lot for automated vehicles based on edge cluster computing. The intelligent parking lot consists of fixed-edge vehicles and moving-edge vehicles, using grid maps for parking management [14]. Siddique et al. (2021) showed how to maximize the number of cars in the parking lot, assuming that the interfering vehicles can be moved by a central controller to provide the best results for small batches with a single entry point and provide a heuristic for larger batches, achieving an 80% increase in parking capacity [15].

The design of an automated parking lot requires careful consideration of the inter-related movement of automated cars. The allocation and selection of parking spaces are crucial in ensuring cars' smooth and efficient movement. Previous studies by scholars have provided significant help for the design and optimization of automated parking lots. For example, Han et al. (2017) calculated the optimal path through the Dijkstra algorithm and sent the assigned location and path information to the driver's mobile phone [16]. For the optimization of the parking space scheme, Zaerpour et al. (2017) proposed and solved a hybrid integer nonlinear model to optimize the system dimension by minimizing the search time and obtaining a closed expression of the minimum search time [9]. Yalcin et al. (2018). derived the bounds of the number of eligible empty cars, developed several search guidance estimation functions, and proposed a heuristic search algorithm to solve a more prominent problem instance [13]. Bahrami et al. (2020) studied parking location choices for automated vehicles based on the arrival and departure times to minimize the number of relocations of automated vehicles [4]. Aiming at the large number of disconnected paths existing in intelligent parking systems, Wang et al. (2020) proposed a rollback strategy with an improved ant colony algorithm for the path planning of AVG intelligent parking systems [17].

Some scholars have also used machine learning to optimize the allocation of parking spaces in automated parking lots. For example, Agostinelli et al. (2019) adopted a deep reinforcement learning method, enabling them to reverse-learn how to solve increasingly difficult states from the target state without specific domain knowledge. In total, 100% of

all test configurations were solved with DeepCubeA, finding the shortest path to the target state 60.3% of the time [18]. M. Wu et al. (2021) first predicted the driver's choice of parking space and then assigned parking spaces to automated vehicles. The Floyd algorithm for the shortest distance is used to determine the route for the self-driving car to reach the parking space [19]. Xie et al. (2022) proposed a collaborative approach based on system-side deep reinforcement learning (DRL) to solve the parking space allocation problem in a large AVP environment, improving the allocation efficiency [1]. Some scholars also use robot platforms to improve the efficiency of parking allocation. For example, Chen et al. (2021) proposed an improved genetic algorithm and a time-enhanced A* path planning algorithm for high-density parking lots. The improved genetic algorithm can effectively search the task execution order and robot assignment and converge to the optimal solution, even in large-scale, complex scenarios [3].

In a high-density automated parking lot, the movement of the automated vehicle needs attention, which is related to whether the automated vehicle will have a collision during parking. Thanks to the development of intelligent network connection and intelligent vehicle technology, multi-vehicle collaborative driving is possible, and the problem of automatic parking trajectory planning is transformed into an optimal control problem [20]. In controlling the data transfer process, Ni et al. (2019) proposed a secure and privacy-protecting automated valet parking protocol that further improves the safety and reliability of automated parking lots [21]. For motion control in automated vehicles, combined with today's new sensors, Jang et al. (2020) proposed a reconfigurable automatic parking system with an independent ambient view monitor. The system can constantly reflect several errors and risks of perception, positioning, and control in the actual scene and then re-generate the parking path, improve the parking accuracy, and avoid collisions [22]. Zhang et al. (2021) used an improved plan-based collaborative driving approach to enable multiple AGVs to travel efficiently in conflict zones without collisions and deadlocks [2]. Kim et al. (2020) believe that, in the future, fully automated vehicles will use various sensors and communication modules to operate in buildings such as indoor parking lots [14].

Studies conducted by scholars have revealed that automatic parking lots can increase parking densities by eliminating lanes or employing robot platforms and better parking allocation algorithms. Nevertheless, automated valet parking can provide a solution to this problem and achieve even greater parking densities. We already have the necessary technology. What we need is efficient parking lot design and planning. However, planning for automated parking has to take into account the transition period between human-driven vehicles (HVs) and automated vehicles (AVs) in the same parking infrastructure [20]. Electric vehicles will be rapidly popularized in the future, so it is necessary to take electric vehicle charge and discharge scheduling as part of parking lot planning and design [23].

Previous studies suggested that automated parking lots were obstacle-free and did not require charging stations. However, with the growth of electric vehicles, it is now crucial to consider the layout of relevant charging facilities. In addition, there is limited research on parking lot designs that accommodate both conventional and automated vehicles. The hybrid parking lot, which caters to both types of vehicles, will become an essential part of future traffic facilities. Zhang et al. think that, in underground parking lot design, it has become necessary to develop and build an underground parking system to relieve the pressure of surface traffic and traffic congestion [24]. Wu et al. believe that with the development of automated valet parking systems, there will be a transition period during which human-driven vehicles (HVs) and autonomous vehicles (AVs) will be present in the same parking infrastructure at the same time [19]. They designed a hybrid parking lot in three different scenarios. Compared with their design, the parking lot designed in our paper achieves a higher capacity and density. Infrastructure-based autonomous driving systems are increasingly being used in confined environments [25]. Compared with traditional human-driven vehicles, AGVs can ensure the uniformity and stability of parking motion. At the same time, it can reduce the space for human entry and exit so that it can achieve more parking capacity and density in the same area of the parking lot.

Therefore, in this paper, we research the high-density layout design of parking lots that cater to self-driving cars, considering obstacles and charging stations. We also explore the high-density layout design of hybrid parking lots that cater to conventional and automated vehicles in varying proportions. Our study differs from the existing literature in two significant ways: first, we develop optimal designs for small parking lots that may have barriers or charging piles, as commonly found in urban settings. Second, we provide better methods for conventional and automated hybrid parking lots, which can serve as a reference for future parking lot designs.

2. Designs of the Parking Lots

2.1. Parking Attributes of Automated Guided Vehicles

In this section, model parameters and variables according to the work requirements are defined in detail. The given parameters and defined variables are described as follows (some of the variables are described in Table 1):

Table 1. Notation.

Symbol	Definition
h	Minimum lateral clear distance
R_s	Radius of the curve inside the driving track of the AGV
W_d	Width of the track to the road edge
θ	Center angle of the stadia line
s	Parking acceleration/deceleration distance
v_1	Initial velocity of parking
v_2	Final velocity of parking
t_A	Startup time of parking
t_B	Steady time of parking
v_s	Acceleration/deceleration speed
m	Number of horizontal grids
n	Number of vertical grids
S_d	Decision space
C	Capacity of parking lots
D	Density of parking lots
S_u	Actual use area of parking
$\delta(c)$	Obstruction coefficient
α	Automated parking lot coefficient
β	Traditional parking lot coefficient

When parking automated guided vehicles (AGV) in a parking lot, it is crucial to consider the driving time, available space, and movement patterns of the cars. During the parking movement, AGVs cannot move horizontally in parallel, and a sufficient turning radius should be considered. This paper outlines the characteristic parameters of the minimum lateral clear distance h required during the parking process.

$$h = R_s - \frac{R_s(R_s - W_d) \sin \theta}{\sqrt{R_s^2 + (R_s - W_d)^2} - 2R_s(R_s - W_d) \cos \theta} \quad (1)$$

Furthermore, this paper elaborates on the key parameters that determine the acceleration and deceleration distance of automated guided vehicles (AGV) in parking scenarios.

$$s = \frac{v_1^2 - v_2^2}{2v_s} + \frac{1}{2}v_1(t_A + t_B) \quad (2)$$

This paper employs two formulas: Formula (1) is used to determine the minimum lateral clear distance required for parking, and Formula (2) is used to assess the acceleration and deceleration distance. These formulas are used to design three fundamental trajectories for automated cars in parking space movement. All complex moving trajectories can be

created by combining these three basic trajectories, and we apply these formulas in the subsequent calculation and design of parking lot density.

For a car's simple forward and backward movement, only one grid is required (refer to Figure 1a). However, a turning radius must be considered for turning, which requires four grids to complete the movement (refer to Figure 1b). Similarly, four grids are needed for lateral movement (refer to Figure 1c). Considering these three basic movement patterns, it is possible to calculate the number of grids required for automated vehicles to enter and exit parking lots efficiently.

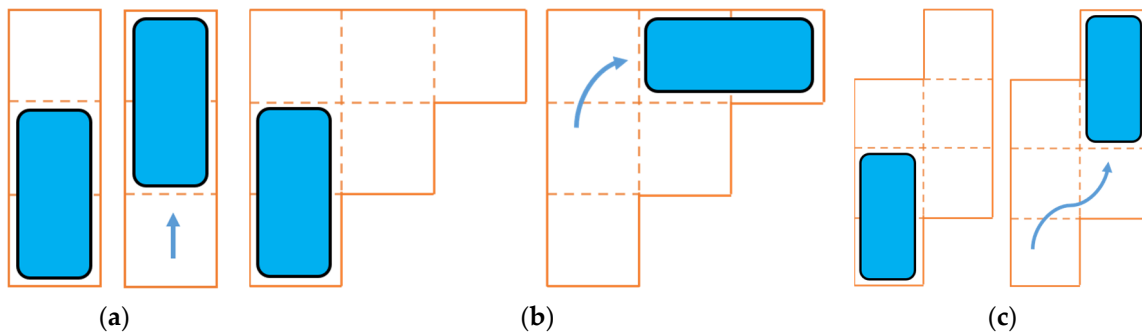


Figure 1. Parking space analysis of vehicles. (a) Dolly moves; (b) Turning; (c) Lateral moves.

2.2. Mobile Priority Environment

To optimize parking space, each vehicle in this study is assigned two grids. The parking lot capacity is designed based on proposed parking characteristics for automated vehicles and three basic moving trajectories. In the case of non-standard-shaped parking lots, several lots can be merged to accommodate them.

This study proposes a mobile priority parking lot where all cars stay parked in the lot. The empty spaces are utilized to move other automated vehicles, making it easier for any car to exit. The parking lot is accessible to both private and public automated vehicles, and all movements must comply with Formulas (1) and (2).

The mobile priority parking lot is analyzed using unique path-driving methods and graph theories. After filling most parking spaces, the remaining space is divided into four scenarios.

m, n are odd and $m, n \geq 3$ (Figure 2a); m is even, n is odd, and $m \geq 4, n \geq 2$ (Figure 2b); m is odd, n is even, and $m \geq 4, n \geq 2$ (Figure 2c); m, n are even, and $m \geq 4, n \geq 2$ (Figure 2d). For example, when the size of a parking lot is 100×98 , its remaining space is the parking space layout, as shown in Figure 2d. This paper focuses on the capacity of mobile priority parking lots, which is determined solely by the remaining decision space S_d in the parking lot. In mobile priority parking lot design, we compute the maximum number of cars that can be parked when both m and n are odd as: the horizontal parking zone has an area of $m(n-3)$ and we park $\frac{m(n-3)}{2}$ cars, the vertical parking zone has an area of, and we park $\frac{3(m-3)}{2}$ cars, and finally 2 cars in the 3×3 base grid, we can park ten cars in the 5×5 base grid. Based on this, a formula for calculating the capacity C_{Avp1} of mobile priority parking lots is derived.

$$C_{Avp1} = \begin{cases} \frac{(m \times n - 5)}{2}, & \text{if both } m \text{ and } n \text{ are odd} \\ \frac{(m \times n - 6)}{2}, & \text{otherwise} \end{cases} \quad (3)$$

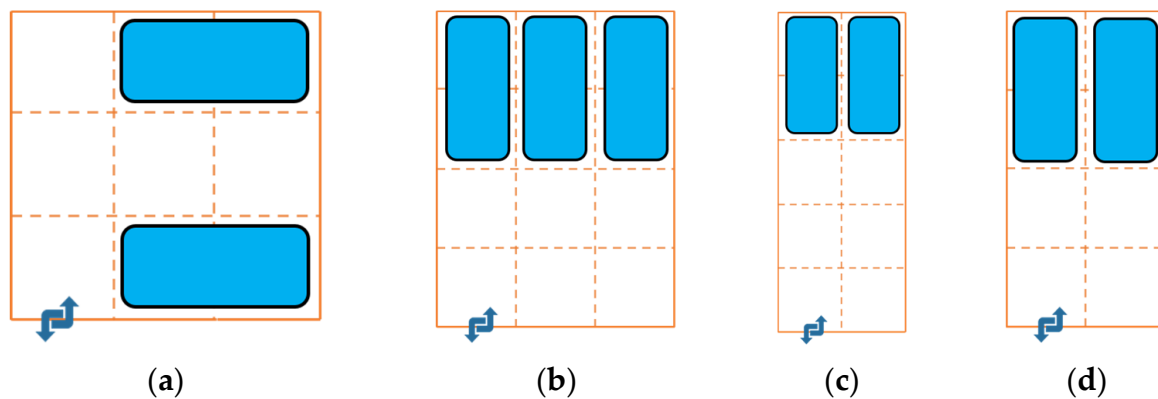


Figure 2. Remaining space of the mobile priority parking lot: (a) 3×3 ; (b) 4×3 ; (c) 5×2 ; (d) 4×2 . The capacity of a parking lot of any size is only related to the remaining space.

According to Formula (3) for mobile priority parking lot capacity, the density formula D_{Avp1} can be deduced as follows:

$$D_{Avp1} = \begin{cases} \frac{(m \times n - 5)}{mn}, & \text{if both } m \text{ and } n \text{ are odd} \\ \frac{(m \times n - 6)}{mn}, & \text{otherwise} \end{cases} \quad (4)$$

According to Formulas (3) and (4), it is possible to perform additional calculations to determine the result.

$$\lim_{m,n \rightarrow \infty} C_{Avp1} = \frac{mn}{2}, \quad \lim_{m,n \rightarrow \infty} D_{Avp1} = 1, \quad \text{if } m \rightarrow \infty, n \rightarrow \infty$$

Based on the findings, it can be inferred that when the parking lot is sufficiently spacious, the parking density of the mobile priority parking area proposed in this research is nearly one, implying that it is almost fully utilized.

2.3. Obstruction Environment

Many cities face limited land resources, which means that parking lots often cannot be built on the surface. This has led to the increasing importance of designing efficient underground parking lots. However, these parking lots often present obstacles such as load-bearing columns or electric vehicle charging stations, which can complicate the movement of vehicles within the lot. To address this, the lot's capacity is designed based on the parking characteristics of automated vehicles and their three basic moving trajectories. If the lot has an irregular shape due to obstacles, it can be made up of several obstacle parking lots with varying specifications.

Compared to the mobile priority parking lot in the obstruction-free scenario in Section 2.2, the automated parking lot with obstacles (as seen in Figure 3a) has higher requirements for vehicle movement during the parking process. In Figure 3b, each size of the obstacle parking lot can be approximated as an $m \times n$ mobile priority parking lot covered with $c = a \times b$ rectangular obstacles (where a represents the number of obstacles on the horizontal side and b represents the number of obstacles on the vertical side). In Figure 3c, the space they occupy cannot be fully utilized due to the length l and width w of the obstacles. In the formula, $\sum_{i=1}^a l_i$ represents the lateral length of the parking lot affected by the obstacle, and $\sum_{i=1}^b w_i$ represents the vertical width of the parking lot affected by the barrier.

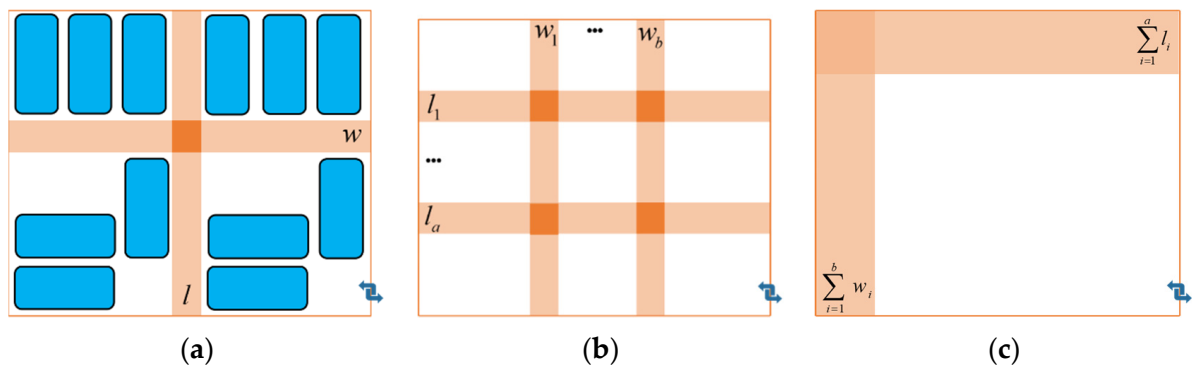


Figure 3. Schematic diagram and actual use area of the parking lot with obstructions. (a) Schematic diagram; (b) Actual use area; (c) Area (adjusted).

Thus, we can further deduce the actual use area formula S_u of the parking lot with obstacles as follows:

$$S_u = \left(m - \sum_{i=1}^a l_i \right) \left(n - \sum_{i=1}^b w_i \right) \tag{5}$$

Using the mobile priority parking lot design from Section 2.2, we will utilize unique path driving methods and graph theories to analyze automated parking with obstacles. For $m \times n$ parking lots, most areas of the parking lot are filled with parked cars. The remaining decision space S_d will be divided into four scenarios.

m, n are odd and $m, n \geq 3$ (Figure 4a), m is even, n is odd, and $m, n \geq 6$ (Figure 4b), m is odd, n is even, and $m, n \geq 6$ (Figure 4c), and m, n are even and $m, n \geq 6$ (Figure 4d). The obstructions for small car parks are usually located on the periphery of the car park. Hence, the remaining decision space for small car parks of the remaining size is consistent with that of accessible car parks. Additionally, the formula for obstruction parking lot capacity in the case of a large parking lot scale C_{Avp2} can be derived from the following:

$$C_{Avp2} = \begin{cases} \frac{(m \times n - 7)}{2}, & \text{if both } m \text{ and } n \text{ are odd} \\ \frac{(m \times n - 8)}{2}, & \text{otherwise} \end{cases} \tag{6}$$

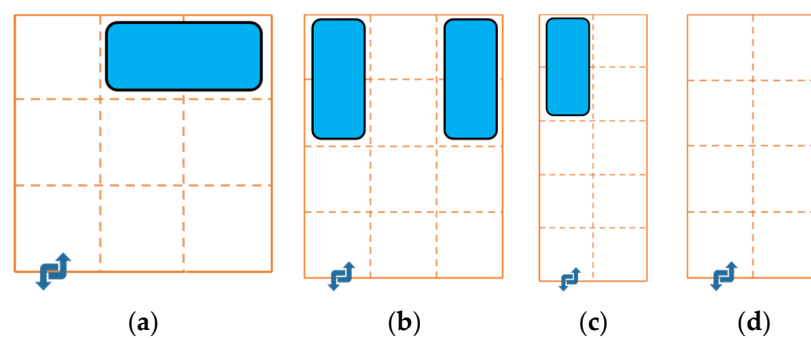


Figure 4. Remaining decision space of a parking lot with obstruction: (a) 3×3 ; (b) 4×3 ; (c) 5×2 ; (d) 4×2 . The capacity of a parking lot of any size is only related to the remaining space.

Formulas (5) and (6) can be used to further deduce the density formula D_{Avp2} of the mobile priority parking lot.

$$D_{Avp2} = \begin{cases} \frac{\left(m \times n - m \sum_{i=1}^b w_i - n \sum_{i=1}^a l_i + \sum_{i=1}^b w_i \sum_{i=1}^a l_i - 7 \right)}{mn}, & \text{if both } m \text{ and } n \text{ are odd} \\ \frac{\left(m \times n - m \sum_{i=1}^b w_i - n \sum_{i=1}^a l_i + \sum_{i=1}^b w_i \sum_{i=1}^a l_i - 8 \right)}{mn}, & \text{otherwise} \end{cases} \tag{7}$$

When there are no obstacles, the obstruction parking lot can be converted to a mobile priority parking lot, and the formula for the obstruction influence coefficient $\delta(c)$ can be derived as:

$$\delta(c) = \begin{cases} 1, & \text{if } c \neq 0 \\ 0, & \text{if } c = 0 \end{cases} \quad (8)$$

Formulas (3), (6), and (8) can be used to deduce the capacity formula C_{Avp} for automated parking lots.

$$C_{Avp} = \begin{cases} \frac{(m \times n - 5 - 2 * \delta(c))}{2}, & \text{if both } m \text{ and } n \text{ are odd} \\ \frac{(m \times n - 6 - 2 * \delta(c))}{2}, & \text{otherwise} \end{cases} \quad (9)$$

Formulas (3), (6), and (8) can be used to deduce the density formula D_{Avp} for automated parking lots.

$$D_{Avp} = \begin{cases} \frac{\left(\frac{m \times n - m \sum_{i=1}^b w_i - n \sum_{i=1}^a l_i + \sum_{i=1}^b w_i \sum_{i=1}^a l_i - 5 - 2 * \delta(c)}{mn} \right)}{\left(\frac{m \times n - m \sum_{i=1}^b w_i - n \sum_{i=1}^a l_i + \sum_{i=1}^b w_i \sum_{i=1}^a l_i - 6 - 2 * \delta(c)}{mn} \right)}, & \text{if both } m \text{ and } n \text{ are odd} \\ \frac{\left(\frac{m \times n - m \sum_{i=1}^b w_i - n \sum_{i=1}^a l_i + \sum_{i=1}^b w_i \sum_{i=1}^a l_i - 6 - 2 * \delta(c)}{mn} \right)}{\left(\frac{m \times n - m \sum_{i=1}^b w_i - n \sum_{i=1}^a l_i + \sum_{i=1}^b w_i \sum_{i=1}^a l_i - 6 - 2 * \delta(c)}{mn} \right)}, & \text{otherwise} \end{cases} \quad (10)$$

According to Formulas (9) and (10), it is possible to perform additional calculations to determine the result.

$$\lim_{m,n \rightarrow \infty} C_{Avp} = \frac{mn}{2}, \quad \lim_{m,n \rightarrow \infty} D_{Avp} = 1, \quad \text{if } m \rightarrow \infty, n \rightarrow \infty$$

Based on the findings in this paper, it can be inferred that automated parking lots can achieve close to full utilization when the parking lot size is large enough. However, smaller parking lots with obstacles are significantly impacted by the number and size of those obstacles, which aligns with real-world observations.

2.4. Hybrid Environment

To develop parking lots in the future, a necessary process will be the hybrid parking of traditional vehicles with automated vehicles. Hybrid parking lots are expected to continue for a long time. The design of these parking lots is based on the parking characteristics of automated vehicles proposed in Section 2.1. The design also considers the three basic movement tracks proposed in Section 2.1, as well as the mobile priority parking lot and the obstruction parking lot proposed in Section 2.3. The design applies the principles of space and time resource conversion in traffic design and the traffic separation principle in traffic control. A hybrid parking lot with a unique shape can be considered as a combination of several specifications of obstruction parking lots and several traditional parking lots. The area of the subarea of the hybrid parking lot is determined by the number of horizontal grids m and vertical grids n of the automated parking lot.

In Figure 5, there is a hybrid parking lot consisting of four sub-areas measuring 15×6 each. The parking lot is divided into 50% automated and 50% conventional areas, and the allocation of parking rights for each sub-area depends on the real-time needs of both automated and conventional vehicles. For example, if there is a higher demand for traditional parking, more sub-areas can be designated for conventional vehicles. This results in variability in the design of the hybrid parking lot sub-area.

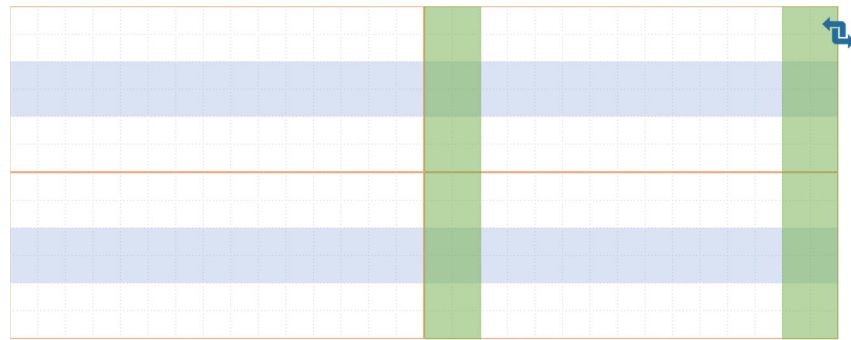


Figure 5. Design of a hybrid parking lot with humans and automated vehicles.

To facilitate research, this paper assumes that the road width of a traditional parking lot occupies two grids (as shown by the green-covered area in Figure 5). If a sub-area is used as an automated parking lot, the blue-covered area can be utilized as a parking space. Conversely, the blue-covered area can be used as a driving road if it is used as a conventional parking lot. The berth layout of the sub-area of the hybrid parking lot is illustrated in Figure 6a,b.

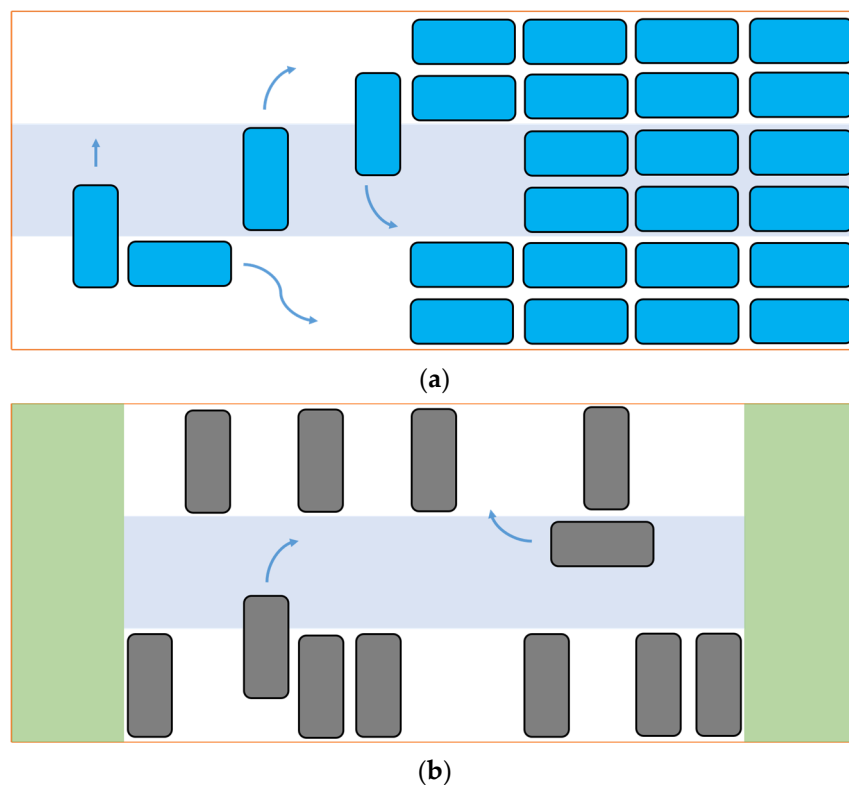


Figure 6. Hybrid parking lot design in sub-areas. (a) Automated subarea; (b) Conventional subarea.

This paper proposes a hybrid parking lot that can be combined with $\alpha * m \times n$ obstacle parking lots and $\beta * m \times n$ traditional parking lots. If no rectangular obstacles exist, the obstacle parking lot can be transformed into a mobile priority parking lot. This allows automated subareas to have decision spaces consistent with the mobile priority or obstacle parking lot. In the calculation of the capacity and density of hybrid parking lots with different mixing proportions, we set the traditional parking lot with obstacles. In the traditional parking lot, we set up a two-grid-width lane for human-driven vehicles on the left and right sides and inside the parking lot. Therefore, the number of horizontal grids

in the traditional parking lot is $\left(m - \sum_{i=1}^a l_i - 4\right)$, and the number of vertical grids in the traditional parking lot is $\left(n - \sum_{i=1}^b w_i - 2 \cdot \frac{n}{3}\right)$. With this, the actual area S_u that a single conventional subarea can use can be calculated more accurately.

$$S_u = \left(m - \sum_{i=1}^a l_i - 4\right) \left(n - \sum_{i=1}^b w_i - 2 \cdot \frac{n}{3}\right) \quad (11)$$

The parking lot capacity and parking density in the calculation process are greatly affected by the limited driving conditions of the road in the conventional subarea. This is due to the impact of the occupied area of the road. As a result, the capacity C_t of the conventional subarea can be further derived.

$$C_t = \begin{cases} \frac{(3m \times n - 12n - (n+1)(m-4) - 6 * \delta(c))}{6}, & \text{if both } m \text{ and } n \text{ are odd} \\ \frac{(3m \times n - 12n - n(m-4) - 6 * \delta(c))}{6}, & \text{otherwise} \end{cases} \quad (12)$$

According to Formula (11), the density of the conventional subregion D_t can be derived.

$$D_t = \frac{\left(3m \times n - 3(m-4) \sum_{i=1}^b w_i - n \sum_{i=1}^a l_i + 3 \sum_{i=1}^b w_i \sum_{i=1}^a l_i - 2n(m-2)\right)}{3mn} \quad (13)$$

Based on the capacity formula of the automated parking lot in Formula (9) and the capacity formula of the conventional parking lot in Formula (12), the capacity of the hybrid parking lot C_h is further derived:

$$C_h = \begin{cases} \alpha \cdot \frac{(m \times n - 5 - 2 * \delta(c))}{2} + \beta \cdot \frac{(3m \times n - 12n - (n+1)(m-4) - 6 * \delta(c))}{6}, & \text{if both } m \text{ and } n \text{ are odd} \\ \alpha \cdot \frac{(m \times n - 6 - 2 * \delta(c))}{2} + \beta \cdot \frac{(3m \times n - 12n - n(m-4) - 6 * \delta(c))}{6}, & \text{otherwise} \end{cases} \quad (14)$$

According to Formulas (10) and (13), the density of the hybrid parking lot D_h can be further derived:

$$D_h = \begin{cases} \frac{\alpha \cdot \left(m \times n - m \sum_{i=1}^b w_i - n \sum_{i=1}^a l_i + \sum_{i=1}^b w_i \sum_{i=1}^a l_i - 5 - 2 * \delta(c)\right)}{(\alpha + \beta)mn} + \frac{\beta \cdot \left(3m \times n - 3(m-4) \sum_{i=1}^b w_i - n \sum_{i=1}^a l_i + 3 \sum_{i=1}^b w_i \sum_{i=1}^a l_i - 2n(m-2)\right)}{3(\alpha + \beta)mn}, & \text{if both } m \text{ and } n \text{ are odd} \\ \frac{\alpha \cdot \left(m \times n - m \sum_{i=1}^b w_i - n \sum_{i=1}^a l_i + \sum_{i=1}^b w_i \sum_{i=1}^a l_i - 6 - 2 * \delta(c)\right)}{(\alpha + \beta)mn} + \frac{\beta \cdot \left(3m \times n - 3(m-4) \sum_{i=1}^b w_i - n \sum_{i=1}^a l_i + 3 \sum_{i=1}^b w_i \sum_{i=1}^a l_i - 2n(m-2)\right)}{3(\alpha + \beta)mn}, & \text{otherwise} \end{cases} \quad (15)$$

According to Formulas (14) and (15), the hybrid parking lot's parking capacity and density are related to the number of automated subareas α and conventional subareas β . If $\alpha \neq 0, \beta = 0, c = 0$, the hybrid parking lot can be transformed into a mobile priority parking lot. If $\alpha \neq 0, \beta = 0, c \neq 0$, the hybrid parking lot can be transformed into the obstruction parking lot. When the size of the parking lot and the proportion of automated subareas are large enough, we can further calculate that:

$$\lim_{m, n \rightarrow \infty} C_h = \frac{mn}{2}, \quad \lim_{m, n \rightarrow \infty} D_h = 1, \quad \text{if } m \rightarrow \infty, n \rightarrow \infty, \frac{\alpha}{\alpha + \beta} \rightarrow 1$$

This paper shows that the hybrid parking lot designed in it has a parking density almost at total capacity, with a value close to 1. The parking capacity and density of small-scale hybrid parking lots are significantly influenced by the conventional subarea, which is consistent with real-world observations.

3. Numerical Experiments and Results

3.1. Motion Rationality Based on Graph Theory

Taking the 7×7 size of the mobile priority parking lot as an example (the analysis process is similar for the automated sub-area of the obstruction parking lot and the hybrid parking lot), according to Formula (3), the mobile priority parking lot capacity is: $(m \times n - 5)/2 = (7 \times 7 - 5)/2 = 22$ (i.e., the first picture in the upper-left corner of Figure 7).

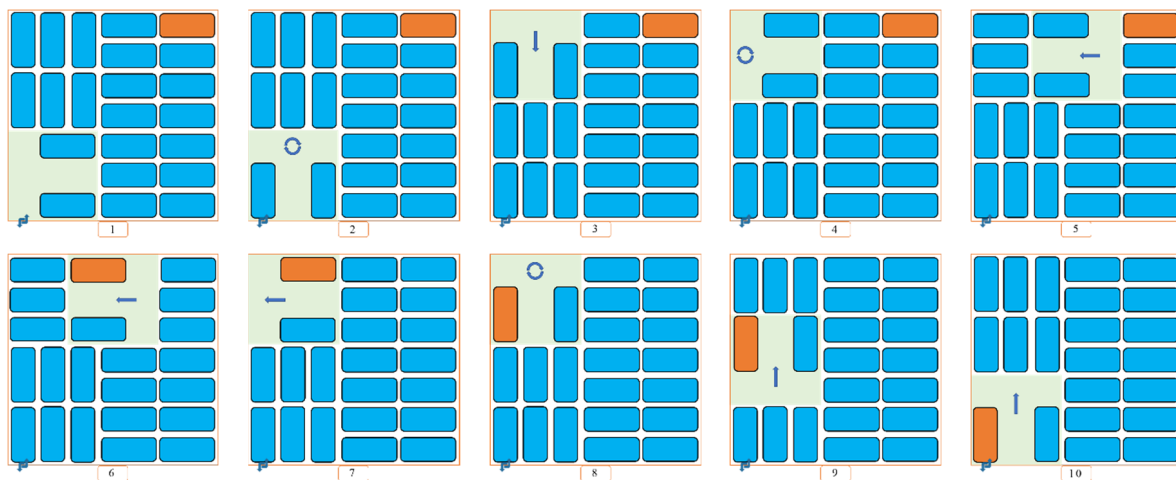


Figure 7. Mobile priority parking lot design and vehicle (orange car) exit method.

Based on the above analysis, the steps for the graph theory analysis of the maximum capacity of the parking lot are as follows:

Step 1: Considering the mobile priority parking, the space that does not affect the entry of the following vehicle and the maximum number of parking vehicles is fully parked, as shown in the two rows of parking on the right of the first picture in Figure 7.

Step 2: There is a remaining decision space of a parking lot conforming to the specifications (the area at the bottom-left corner of the first picture in Figure 7). In the remaining decision space, considering the movement of cars, the parking space is full of vehicles, as shown in the top-left corner of the first picture in Figure 7.

Step 3: Fill the remaining decision space form (Figure 2) into the empty position, as shown in the area at the bottom-left corner of the first picture in Figure 7.

Step 4: By using the residual decision space in the area at the bottom-left corner of the first picture in Figure 7, other automated vehicles are moved to realize the departure of any car in the parking lot.

The conversion process of parking space from the fifth to the sixth in Figure 7 is relatively complicated, and its change process is now explained in detail. The specific entry and exit mode of vehicles in this scheme (the red car leaves) is shown in Figure 8:

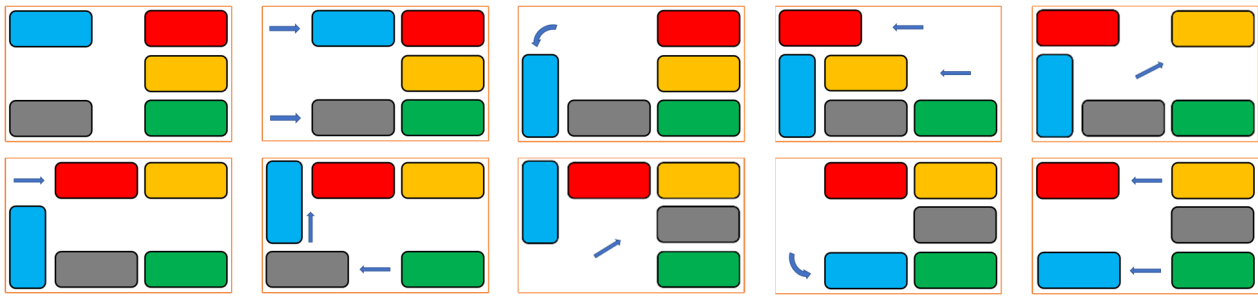


Figure 8. Specific move process.

3.2. Capacity and Density Numerical Validation

To verify the effectiveness of the parking lot design mentioned in this paper, according to the parking lot layout design simulation experiment, the hybrid parking lot with different sizes and combinations based on Formulas (14) and (15) and the traditional underground parking lot were analyzed and compared by a computer programming experiment. To facilitate the calculation of parking lot capacity and parking density, the parking lot involved in the following analysis is composed of four sub-areas (i.e., $\alpha + \beta = 4$), each subarea with obstructions contains two obstructions, and the obstruction size is 1 grid \times 1 grid (i.e., $c = a \times b = 2, l = 1, w = 1$) Three combination schemes are set for the hybrid parking lot ($\alpha : \beta = 3 : 1, \alpha : \beta = 1 : 1, \alpha : \beta = 1 : 3$).

Figure 9 shows the optimization effect of the parking lot designed in this paper on the capacity improvement of the parking lot at different scales. In the 6×6 specification subarea, compared with the 12 vehicles in the traditional parking lot, the parking capacity (dark blue curve shown in Figure 9) of the mobile priority parking lot contains 60 vehicles, the capacity increases by 400%, and the parking capacity (red curve shown in Figure 9) of the hybrid parking lot ($\alpha : \beta = 1 : 3$) is 27 vehicles, and the capacity increases by 125%. In the 12×12 specification subarea, compared with 124 vehicles in the traditional parking lot, the parking capacity (dark blue curve shown in Figure 9) of the mobile priority parking lot design is 276 vehicles, with a capacity increase of 122.58%; the parking capacity (red curve shown in Figure 9) of the hybrid parking lot ($\alpha : \beta = 1 : 3$) is 165 vehicles, with a capacity increase of 33.06%. As the size of the parking lot continues to increase, the increase rate (slope of the curve in Figure 9) of the parking capacity of the five parking lot models involved in this paper continues to rise, and the traditional parking lot is also consistent with the reality due to the restrictions of roads and obstructions in the field.

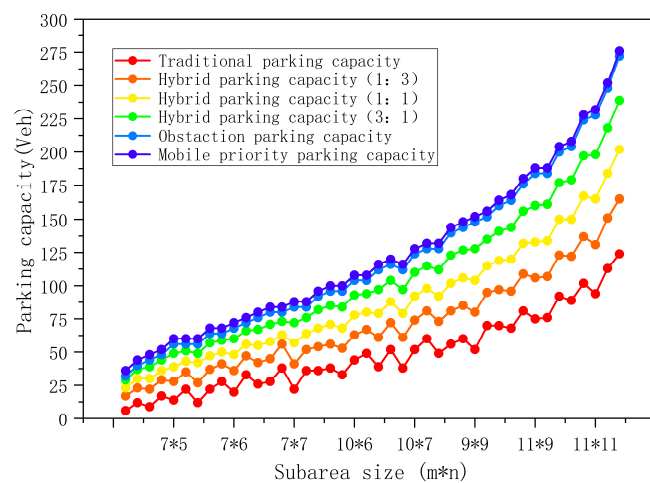


Figure 9. Comparison of parking capacities of different sizes.

Figure 10 shows the optimization effect of the automated parking lot designed in this paper on improving the parking lot density at different scales. Under the 12×12

specification subarea, the parking density (blue curve shown in Figure 10) of the traditional parking lot is 0.35, and the parking density (red curve shown in Figure 10) of the mobile priority parking lot design is 0.96, with a density increase of 174.28%. The parking density (orange curve shown in Figure 10) of the obstruction parking lot is 0.71, with a density increase of 102.85%.

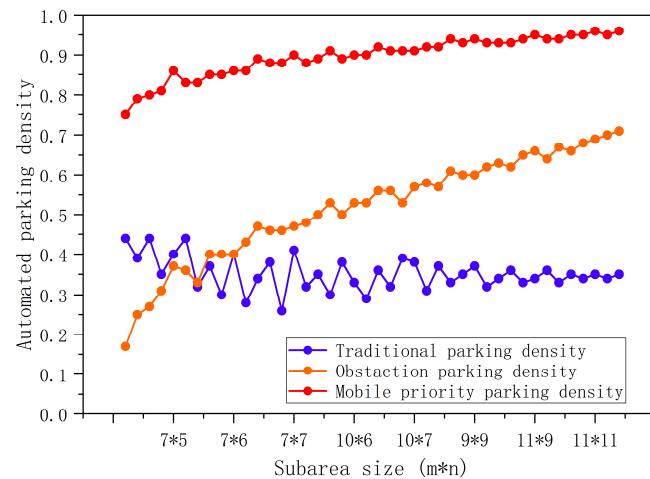


Figure 10. Comparison of the density of automated parking lots.

When the parking lot size is small, the area of obstruction is more significant than that of the parking lot with obstructions, resulting in a smaller available parking area and lower parking density. However, as the size of the parking lot $m \times n$ continues to increase, the proportion of the area of fixed obstructions relative to the obstruction parking lot decreases. The parking density of the obstruction parking lot will continue to rise, exceeding the density of the traditional parking lot in the 7×6 scale subarea (where the orange curve intersects with the blue curve in Figure 10). When the size of the parking lot $m \times n$ is large enough, we can further calculate that:

$$\begin{aligned} \lim_{m,n \rightarrow \infty} D_t &= 0.35 \\ \lim_{m,n \rightarrow \infty} C_{Avp1} &= \lim_{m,n \rightarrow \infty} C_{Avp2} = \frac{mn}{2} \\ \lim_{m,n \rightarrow \infty} D_{Avp1} &= \lim_{m,n \rightarrow \infty} D_{Avp2} = 1.00 \end{aligned}$$

The parking density of the traditional parking lot is close to 0.35, and the parking density D_{avp} of the two automated parking lots designed in this paper is close to 1, which is close to the entire utilization state.

Figure 11 shows the optimization effect of the hybrid parking lot designed in this paper on improving the parking lot density under different mixing ratios and scales. Under the 12×12 specification subarea, the parking density (Figure 11 dark blue curve) of the traditional parking lot is 0.35. The parking density (red curve in Figure 11) of the hybrid parking lot ($\alpha : \beta = 1 : 3$) is 0.57, and the capacity is increased by 62.86%; the parking density (green curve shown in Figure 11) of the hybrid parking lot ($\alpha : \beta = 1 : 1$) is 0.70, and the capacity is increased by 100%; and the parking density (light blue curve shown in Figure 11) of the hybrid parking lot ($\alpha : \beta = 3 : 1$) is 0.83, and the capacity is increased by 137.14%.

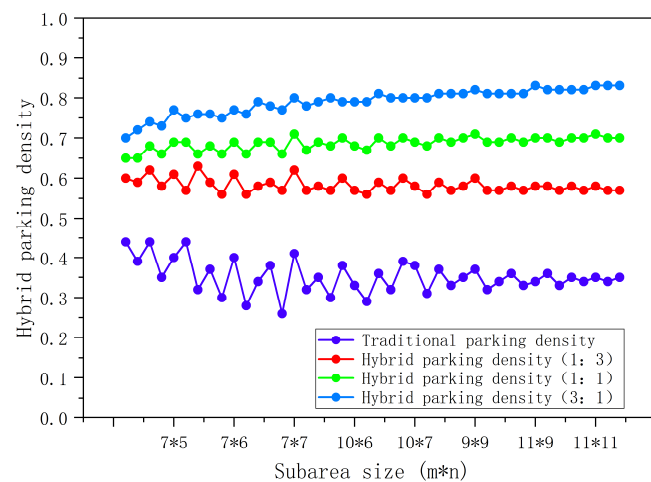


Figure 11. Comparison of the density of hybrid parking lots (in different mixing ratios).

When the parking lot size $m \times n$ is small, the parking density of the three hybrid parking lots is close to each other. As the proportion of automated parking lots keeps increasing, the overall parking density of the hybrid parking lot also increases. As the parking lot subarea size $m \times n$ gradually increases, it can be seen that the parking density of the hybrid parking lot tends to be stable. Further, we can calculate that:

$$\lim_{\substack{\alpha : \beta = 1 : 3 \\ m, n \rightarrow \infty}} D_{m1} = 0.57 \quad \lim_{\substack{\alpha : \beta = 2 : 2 \\ m, n \rightarrow \infty}} D_{m2} = 0.70 \quad \lim_{\substack{\alpha : \beta = 3 : 1 \\ m, n \rightarrow \infty}} D_{m3} = 0.83$$

Therefore, compared with the traditional parking lot, the capacity and density of the parking lot designed in this paper have improved significantly, and the optimization effect is better.

3.3. Cause of Curve Oscillation

For the parking lot design with the same number of grids, different parking lot capacities and densities are presented due to the difference between the number of horizontal grids, the number of vertical grids, and the occupied area of obstacles and roads. According to the previous setting, the parking lot is composed of four sub-areas (i.e., $\alpha + \beta = 4$), taking the parking lot with a hybrid parking lot of an automated sub-area and conventional sub-area as an example ($\alpha : \beta = 1 : 1$).

The superposition of sub-areas is applied to explain the impact on the parking lot's capacity. The total number of grids of one 9×8 scale parking lot and two 9×4 scale parking lots is the same. Still, the remaining decision space exists in both sub-areas, resulting in the density and capacity of the stacked parking lot being less than that of an integral one. When the two automated sub-areas are superimposed, they are merged into a large-scale automated sub-area to maximize the number of parking lots. As shown in Figure 12.

For the sub-area containing 36 grids, there are two different layout methods: the sub-area of a 9×4 scale and the sub-area of a 6×6 scale. The following figure is the design of the hybrid parking lot under the sub-area of the 9×4 scale. As shown in Figure 13.

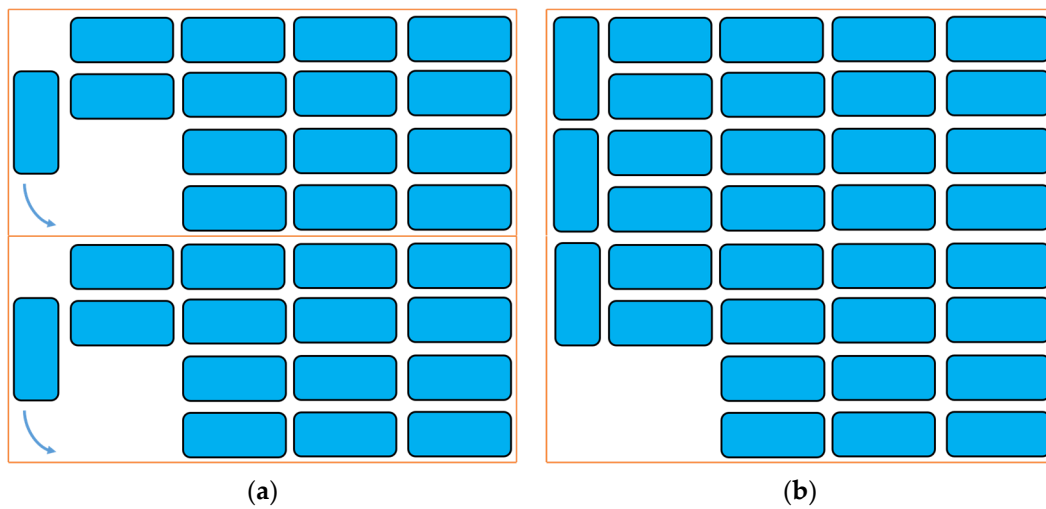


Figure 12. The influence of area superposition on the capacity and density of the parking lot: (a) $2 \times 9 \times 4$ scale parking lot (30 vehicles); (b) 9×8 scale parking lot (33 vehicles).

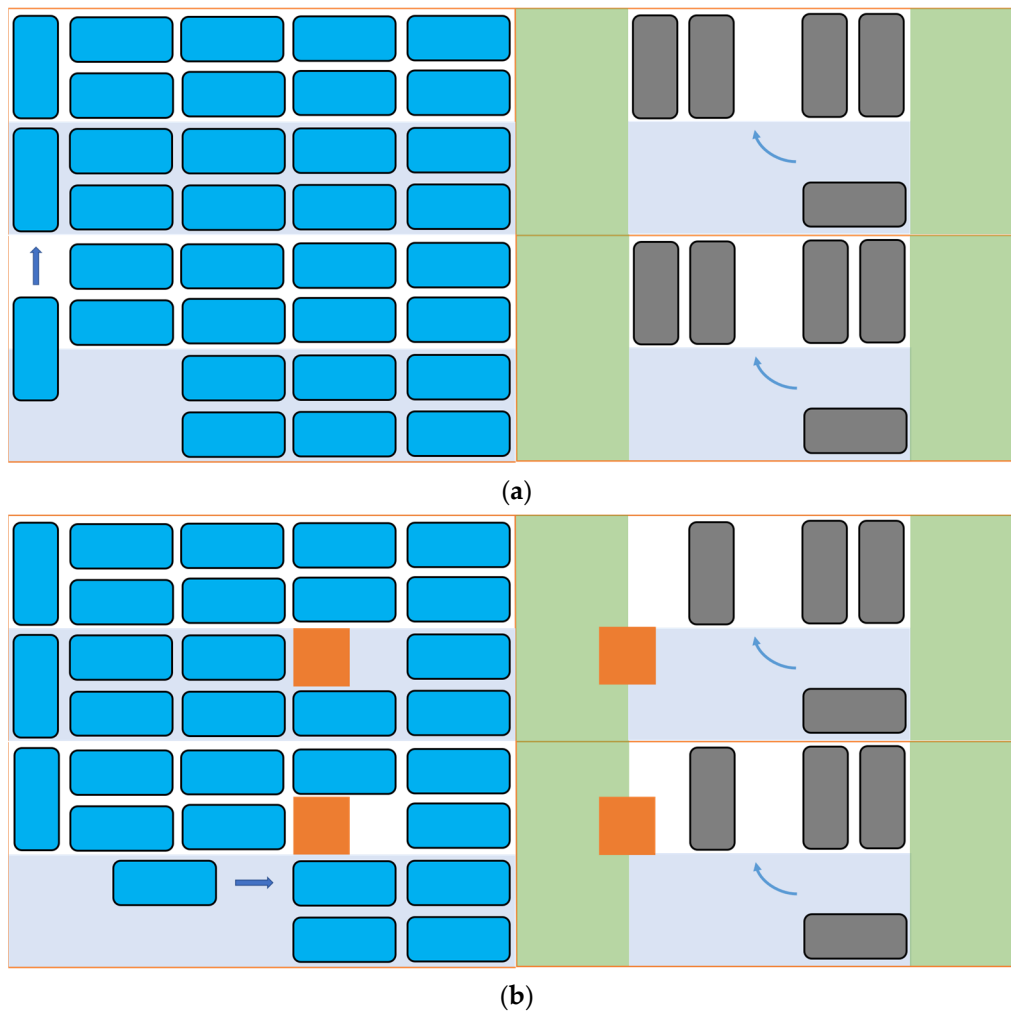


Figure 13. Parking lot under the sub-area of a 9×4 scale. (a) $4 \times 9 \times 4$ scale parking lot (43 vehicles); (b) $4 \times 9 \times 4$ scale parking lot with obstacles (38 vehicles).

The following Figure 14 is the design of the hybrid parking lot under the 6×6 scale subarea.

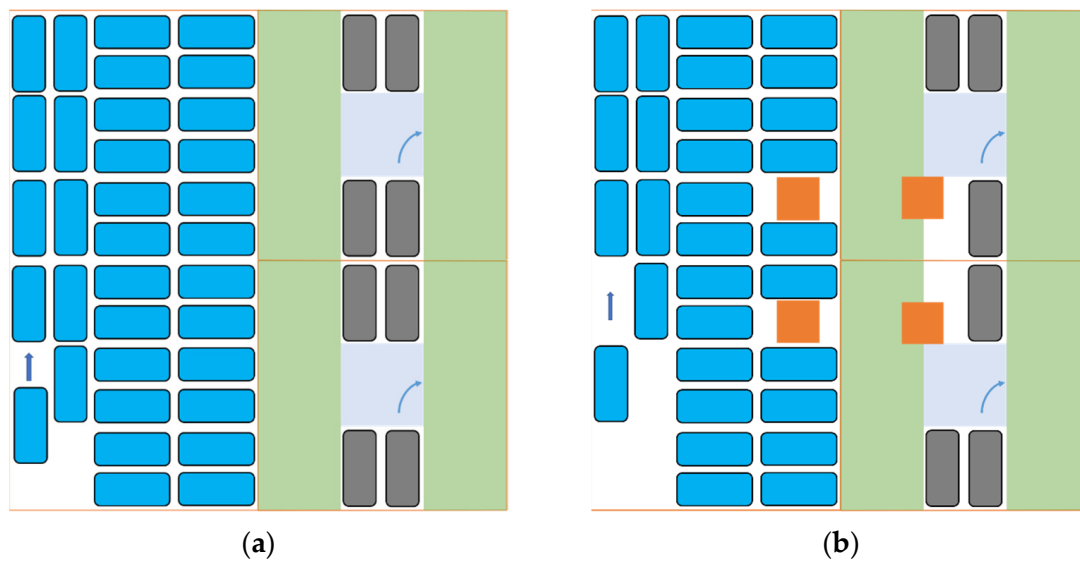


Figure 14. Parking lot under the sub-area of a 6×6 scale. (a) $4 \times 6 \times 6$ scale parking lot (42 vehicles); (b) $4 \times 6 \times 6$ scale parking lot with obstacles (36 vehicles).

As can be seen from the figure, parking lots of a 9×4 scale (43 vehicles), 9×4 scale (38 vehicles in the obstacle scene), 6×6 scale (42 vehicles), and 6×6 scale (36 vehicles in the obstacle scene) have different parking capacities in the same subarea containing 36 grids. The oscillation will be more evident if the parking lot scale is small and contains fixed obstacles (as shown in the figure). With the continuous increase in the scale of the subarea of the parking lot, the oscillation amplitude of the capacity and density will also decrease due to the decrease in the proportion of the area occupied by the obstacles and roads in the subarea, and the density curve will also tend to a stable value.

4. Discussion

Our paper proposes the optimal design of high-density hybrid parking in different scenarios, including the mobile priority parking lot, the parking lot with obstacles, and the hybrid parking lot with human-driven and automated vehicles. We provide examples of three different mixed-ratio parking lot designs and calculate the effectiveness of six parking lot models discussed in the paper. Compared to traditional parking lot models, the proposed parking lot design has significantly improved capacity and density. We present experimental results and provide suggestions for high-density parking lots in multiple scenarios in the future.

In the past, researchers have mainly focused on studying high-density parking in barrier-free and automated scenarios. However, our paper takes into account the design of an underground parking lot that includes building load bearing, the increasing demand for charging stations, and the scenario of a hybrid driving parking lot that will exist for a long time in the future. Therefore, to calculate the capacity and density, we have developed a parking lot design that is similar to realistic scenarios. We have proposed a high-density parking model in our paper, which we have compared with a realistic parking model, and we have drawn a conclusion based on our findings.

Due to the presence of obstacles, the number of vehicles in both the horizontal and vertical areas will be affected. Therefore, parking lots with obstacles will be affected in terms of capacity and density, which is very influential for small-scale parking lots. So, the formula we set up will have a more significant impact when the size of the parking lot is small. The design of the parking lot with obstacles is related to the location of the barriers. We arrange the obstacles under the assumed position to obtain the formula of the parking lot with barriers proposed in the paper.

The formula proposed in this paper becomes more accurate as the size of the parking lot increases. For hybrid parking lot designs, different sub-areas can be mixed to create a parking lot of various shapes and sizes. Due to variations in the sub-areas, scale, and quantity, we provide a formula for calculating hybrid parking lots. For parking lots with irregular shapes, it is necessary to divide the parking lot into smaller sub-areas and conduct a proportional analysis for each area to obtain accurate results. In the result presentation section of the paper, we provide three rectangular parking lot designs to verify the model.

This paper provides the optimal design of a planar high-density parking lot. However, for a high-density parking lot that is quickly filled with vehicles, it takes a lot of time to make the cars inside move out, so it is worth further research on the algorithm of parking space allocation. It is important to note that a three-dimensional parking lot cannot be viewed as a simple flat stack. It is necessary to also consider the movement and positioning of the vehicle, as this will impact the safety and efficiency of parking.

5. Conclusions

This paper innovatively proposes the design of a mobile priority parking lot based on the parking attributes of automated vehicles, which can optimize the maximum capacity of automated vehicles. Based on the mobile priority parking lot and considering the distribution of obstructions in the underground parking lot, the optimized design of the parking lot with obstructions is further proposed, which can better solve the impact of charging piles and indoor building-bearing columns on the parking of automated vehicles. Based on the spatiotemporal resource conversion in traffic design and the principle of traffic separation in traffic control, this paper designs a mobile priority parking lot, proposes an optimized design of a hybrid parking lot with conventional and automated vehicles, and improves the utilization rate of parking lots through the variability of parking areas to maximize the capacity and density of urban parking lots in different scenarios. In this paper, we propose a multi-scene high-density parking design, which is more in line with the situation in real life than previous studies on high-density parking by scholars. This paper is innovative in studying complex scenarios, such as hybrid high-density parking lots with obstacles such as load-bearing columns and charging piles. The following conclusions are obtained through the analysis of numerical examples:

(1) The capacity and density of a parking lot depend on various factors, including the design, number, size, and mixing ratio of obstacles. It is important to note that the number, size, and mixing ratio of obstacles play a significant role in determining a parking lot's parking capacity and density.

(2) For automated parking lots, that is, mobile priority parking lots and parking lots with obstructions, with the continuous increase in the scale of sub-areas, the parking density will approach one, approximately reaching the entire utilization state.

(3) For parking lots with human drivers, such as traditional parking lots and hybrid parking lots (with different mixing ratios), with the continuous increase in the size of sub-areas, the maximum density of various hybrid parking lots will tend to be a fixed value, so in the future design process of hybrid parking lots, we should not only consider the scale construction but also consider the impact of the mixing ratio on the capacity and density of parking lots.

When trying to increase the number of parking spaces in urban areas, it may be helpful to refer to the parameter design outlined in this paper. As automated vehicle technology advances and land resources become more limited, future research will focus on maximizing capacity and efficiency in three-dimensional parking structures for different scenarios.

Author Contributions: T.C.: Study conception and design; draft manuscript preparation. C.S.: The testing of examples; paper revision. All authors have read and agreed to the published version of the manuscript.

Funding: Humanities and Social Sciences Foundation of the Ministry of Education of China (No. 22YJCZH153); Universities Philosophy and Social Science Research of Jiangsu Province (No. 2022SJYB2221).

Institutional Review Board Statement: Not applicable.

Informed Consent Statement: Not applicable.

Data Availability Statement: Not applicable.

Conflicts of Interest: The authors declare no conflict of interest.

References

1. Xie, J.; He, Z.; Zhu, Y. A DRL based cooperative approach for parking space allocation in an automated valet parking system. *Appl. Intell.* **2022**, *53*, 5368–5387. [[CrossRef](#)]
2. Zhang, J.; Li, Z.; Li, L.; Li, Y.; Dong, H. A bi-level cooperative operation approach for AGV based automated valet parking. *Transp. Res. Part C Emerg. Technol.* **2021**, *128*, 103140. [[CrossRef](#)]
3. Chen, G.; Hou, J.; Dong, J.; Li, Z.; Gu, S.; Zhang, B.; Knoll, A. Multiobjective Scheduling Strategy With Genetic Algorithm and Time-Enhanced A* Planning for Autonomous Parking Robotics in High-Density Unconventional Parking Lots. *IEEE/ASME Trans. Mechatron.* **2021**, *26*, 1547–1557. [[CrossRef](#)]
4. Bahrami, S.; Roorda, M.J. Autonomous vehicle relocation problem in a parking facility. *Transp. A Transp. Sci.* **2020**, *16*, 1604–1627. [[CrossRef](#)]
5. Kang, D.; Hu, F.; Levin, M.W. Impact of automated vehicles on traffic assignment, mode split, and parking behavior. *Transp. Res. Part D Transp. Environ.* **2022**, *104*, 103200. [[CrossRef](#)]
6. Zakharenko, R. Self-driving cars will change cities. *Reg. Sci. Urban Econ.* **2016**, *61*, 26–37. [[CrossRef](#)]
7. Millard-Ball, A. The autonomous vehicle parking problem. *Transp. Policy* **2019**, *75*, 99–108. [[CrossRef](#)]
8. Ferreira, M.; Damas, L.; Conceicao, H.; d’Orey, P.M.; Fernandes, R.; Steenkiste, P. Self-Automated Parking Lots for Autonomous Vehicles based on Vehicular Ad Hoc Networking. Presented at the IEEE Intelligent Vehicles Symposium (IV), Dearborn, MI, USA, 8–11 June 2014.
9. Zaerpour, N.; Yu, Y.; de Koster, R. Small is Beautiful: A Framework for Evaluating and Optimizing Live-Cube Compact Storage Systems. *Transp. Sci.* **2017**, *51*, 34–51. [[CrossRef](#)]
10. Nourinejad, M.; Bahrami, S.; Roorda, M.J. Designing parking facilities for autonomous vehicles. *Transp. Res. Part B Methodol.* **2018**, *109*, 110–127. [[CrossRef](#)]
11. Azevedo, J.; D’Orey, P.M.; Ferreira, M. High-Density Parking for Automated Vehicles: A Complete Evaluation of Coordination Mechanisms. *IEEE Access* **2020**, *8*, 43944–43955. [[CrossRef](#)]
12. Naji, B.; Abdelmoula, C.; Masmoudi, M. A Real Time Algorithm for Versatile Mode Parking System and Its Implementation on FPGA Board. *Appl. Sci.* **2022**, *12*, 655. [[CrossRef](#)]
13. Yalcin, A.; Koberstein, A.; Schocke, K.-O. An optimal and a heuristic algorithm for the single-item retrieval problem in puzzle-based storage systems with multiple escorts. *Int. J. Prod. Res.* **2018**, *57*, 143–165. [[CrossRef](#)]
14. Kim, W.; Jung, I. Smart Parking Lot Based on Edge Cluster Computing for Full Self-Driving Vehicles. *IEEE Access* **2022**, *10*, 115271–115281. [[CrossRef](#)]
15. Siddique, P.J.; Gue, K.R.; Usher, J.S. Puzzle-based parking. *Transp. Res. Part C Emerg. Technol.* **2021**, *127*, 103112. [[CrossRef](#)]
16. Han, Y.; Shan, J.; Wang, M.; Yang, G. Optimization design and evaluation of parking route based on automatic assignment mechanism of parking lot. *Adv. Mech. Eng.* **2017**, *9*, 1687814017712416. [[CrossRef](#)]
17. Wang, X.; Shi, H.; Zhang, C. Path Planning for Intelligent Parking System Based on Improved Ant Colony Optimization. *IEEE Access* **2020**, *8*, 65267–65273. [[CrossRef](#)]
18. Agostinelli, F.; McAleer, S.; Shmakov, A.; Baldi, P. Solving the Rubik’s cube with deep reinforcement learning and search. *Nat. Mach. Intell.* **2019**, *1*, 356–363. [[CrossRef](#)]
19. Wu, M.; Jiang, H.; Tan, C.-A. Automated Parking Space Allocation during Transition with both Human-Operated and Autonomous Vehicles. *Appl. Sci.* **2021**, *11*, 855. [[CrossRef](#)]
20. Wu, B.; Qian, L.; Lu, M.; Qiu, D.; Liang, H. Optimal control problem of multi-vehicle cooperative autonomous parking trajectory planning in a connected vehicle environment. *IET Intell. Transp. Syst.* **2019**, *13*, 1677–1685. [[CrossRef](#)]
21. Ni, J.; Lin, X.; Shen, X. Toward Privacy-Preserving Valet Parking in Autonomous Driving Era. *IEEE Trans. Veh. Technol.* **2019**, *68*, 2893–2905. [[CrossRef](#)]
22. Jang, C.; Kim, C.; Lee, S.; Kim, S.; Lee, S.; Sunwoo, M. Re-Plannable Automated Parking System With a Standalone Around View Monitor for Narrow Parking Lots. *IEEE Trans. Intell. Transp. Syst.* **2020**, *21*, 777–790. [[CrossRef](#)]
23. Mirzaei, M.J.; Kazemi, A. A dynamic approach to optimal planning of electric vehicle parking lots. *Sustain. Energy Grids Netw.* **2020**, *24*, 100404. [[CrossRef](#)]

24. Zhang, P.; Chen, Z.L.; Liu, H. Study on the layout method of Urban underground parking system—a case of underground parking system in the Central business District in linping New City of Hangzhou. *Sustain. Cities Soc.* **2019**, *46*, 101404. [[CrossRef](#)]
25. Zhao, C.; Song, A.D.; Zhu, Y.F.; Jiang, S.C.; Liao, F.X.; Du, Y.C. Data-Driven Indoor Positioning Correction for Infrastructure-Enabled Autonomous Driving Systems: A Lifelong Framework. *IEEE Trans. Intell. Transp. Syst.* **2023**, *24*, 3908–3921. [[CrossRef](#)]

Disclaimer/Publisher’s Note: The statements, opinions and data contained in all publications are solely those of the individual author(s) and contributor(s) and not of MDPI and/or the editor(s). MDPI and/or the editor(s) disclaim responsibility for any injury to people or property resulting from any ideas, methods, instructions or products referred to in the content.